Journal of Quantitative Spectroscopy & Radiative Transfer 111 (2010) 634–642

Contents lists available at ScienceDirect

Journal of Quantitative Spectroscopy & Radiative Transfer

journal homepage: www.elsevier.com/locate/jqsrt

A new 1D approximation for the solution of 2D radiative transfer problems

O.V. Nikolaeva [a], L.P. Bass [a], V.S. Kuznetsov [b], A.A. Kokhanovsky [c,d,*]

[a] Keldysh Institute of Applied Mathematics, Russian Academy of Science, Moscow, Russia
[b] Research Scientific Center "Kurchatov Institute", Moscow, Russia
[c] Institute of Remote Sensing, Bremen University, O. Hahn Allee 1, Bremen, Germany
[d] Institute of Physics, National Academy of Sciences of Belarus, Pr. Nezavisimosti 68, Minsk, Belarus

ARTICLE INFO

Article history:
Received 29 July 2009
Received in revised form
31 October 2009
Accepted 3 November 2009

Keywords:
Radiative transfer
Clouds
3D effects

ABSTRACT

The simplified M-1D algorithm (M stands for modified) for the calculation of horizontal distribution of reflected brightness coefficient in 2D regions with large homogeneous pixels is presented. This algorithm is based upon modified 3^*N-1 1D-transport equations (where N is the number of large pixels) instead of one 2D-transport equation, usually used in such problems. The method does not rely on empiric assumptions on both optical properties of atmosphere or diffuse radiation intensity. Numerical results demonstrating the accuracy of the presented algorithm for simulating brightening and shadowing effects in a vicinity of the jump of optical properties given. The accuracy of the M-1D approximation strongly depends on the geometry and illumination conditions. However, it remains below 15% and can reach 1% for all cases studied and is strongly higher than the accuracy of usually employed independent pixel approximation. Time reduction via replacing 2D problem via modified 1D problem is about 17 times for all cases considered in this paper.

1. Introduction

Clouds are for sure 3D objects. They have finite vertical and horizontal dimensions and also they have quite a complex internal structure. Therefore, their properties can be correctly estimated both in forward and inverse problems only with the application of 3D radiative transfer equation [1]. Nevertheless, the application of this equation to the solution of forward and especially inverse atmospheric optics problems in a cloudy atmosphere is not widespread (see, e.g., [2]). This is mostly due to the fact that the speed of numerical calculations is so low in this case that only a limited number of problems can be solved. In particular, modern satellite retrieval algorithms are entirely based on the 1D radiative transfer theory assuming that clouds have infinite horizontal extent and their properties do not vary in the horizontal direction. Clearly, it leads to known biases in the retrieved cloud parameters [1].

We pose the following question—is it possible to reduce the general 3D equation to a system of 1D equations? Clearly, the answer is negative as far as the exact solution of the problem is of concern. However, the approximate solution of the reduction problem (with varying degree of accuracy dependent on the geometry and the problem at hand) is possible. To show this is the main task and idea of this publication. For the simplicity, only the reduction of 2D case (when both optical properties of atmosphere and radiation intensity depend on height and one horizontal coordinate) to the system of 1D equations (where a solution depends on one spatial coordinate) is considered in details. Note that adding one more dimension (3D, when all functions depend on all

* Corresponding author at: Institute of Remote Sensing, Bremen University, O. Hahn Allee 1, Bremen, Germany.
E-mail address: alexk@iup.physik.uni-bremen.de (A.A. Kokhanovsky).

0022-4073/$ - see front matter © 2009 Elsevier Ltd. All rights reserved.
doi:10.1016/j.jqsrt.2009.11.008

three spatial coordinates) does not bring additional complications in the general approach described below.

The equations derived are more superior with respect to usually applied approach to the treatment of 2D systems such as broken cloud fields based on the independent pixel approximation (IPA). IPA is widely used to simulate radiative transfer in the atmosphere. However, the results of IPA can be quite misleading under strongly horizontally varying optical properties of the media. Such variations are feature of broken clouds systems, where horizontal radiation transport, caused by horizontally varying optical properties impacts essentially the coefficient of brightness of reflected, transmitted and also absorbed solar light.

We consider 2D spatial regions, consisted of two large pixels, where the light intensity depends on two spatial variables—height and horizontal coordinate—and hence can be defined in the framework of 2D geometry by a special choice of the coordinate system (Section 2). Modified M-1D model under consideration is outlined in Section 3. This model is based upon averaging the 2D transport equation over spatial coordinates [3,4], for both height and horizontal. It does not rely on any empirical assumptions on optical and geometrical properties of pixels and radiation intensity in contrast to the other approximate models for treating the horizontal radiation transfer (for example, [5]). It aimed at calculation of the brightness coefficient rather than the mean radiative characteristics in statistically inhomogeneous cloud fields.

To solve all transport problems (both 2D and 1D), the discrete ordinate method and successive-orders-of-scattering (SOS) iteration process with the diffusion-synthetic acceleration (DSA) method [6,7] are used (Section 4). This is not the best method of solution in all cases. Clearly, the most rapid calculation can be done by an analytical method, based upon analytical solutions of the discrete ordinate differential equations. But the construction of new effective numerical algorithms is not a subject of this paper. This paper is aimed at probing and testing a new approach for solving 2D transport problem via a system of modified 1D transport equations. The numerical results showing good accuracy of the presented M-1D method for solving 2D problems are presented in Section 4.

2. 2D transport problem

Let us consider a spatial region composed of two large homogeneous zones, see Fig. 1, with very different optical properties (for example, cloud and clear sky). Both zones are illuminated by solar light beam, directed perpendicular to the boundary of the zones, see Fig. 1. Then intensity of diffuse solar light can be found via the two-dimensional radiation transport equation:

$$\xi\frac{\partial I(x,z,\theta,\varphi)}{\partial x}+\gamma\frac{\partial I(x,z,\theta,\varphi)}{\partial z}+\sigma_{\mathrm{ext}}(x)I(x,z,\theta,\varphi)$$
$$=\frac{1}{4\pi}\sigma_{\mathrm{sca}}(x)\int_0^{\pi}\sin\theta'\,d\theta'\int_0^{2\pi}I(x,z,\theta',\varphi')p(x,\chi(\theta,\varphi,\theta',\varphi'))\,d\varphi'$$
$$+Q(x,z,\theta,\varphi,\Theta,\Phi)F_0. \quad (1)$$

Here

$$\xi=\sin\theta\cos\varphi,\quad \gamma=\cos\theta,$$
$$\chi(\theta,\varphi,\theta',\varphi')$$
$$=\cos\theta\cos\theta'+\sin\theta\sin\theta'\cos(\varphi-\varphi'),$$

$$-x_L<x<x_R,\quad 0<z<H,\quad 0<\theta<\pi,\quad 0<\varphi<2\pi.$$

Function $I(x,z,\theta,\varphi)$ in Eq. (1) defines diffuse radiation intensity at spatial point (x,z) of the 2D region $-x_L<x<x_R$, $0<z<H$ in direction $\vec{\Omega}$, determined by angles (θ,φ), see Fig. 1. Functions $\sigma_{\mathrm{ext}}(x)$, $\sigma_{\mathrm{sca}}(x)$ are extinction and scattering coefficients. Scattering phase function $p(x,\chi)$ is normalized by the following relation:

$$\frac{1}{4\pi}\int_0^{\pi}d\theta'\sin\theta'\int_0^{2\pi}d\varphi' p(x,\theta,\varphi,\theta',\varphi')=1.$$

The source $Q(x,z,\theta,\varphi,\Theta,\Phi)$ describes the generation of diffuse light from the direct sunlight, incident on the top boundary z=0 at the zenith angle Θ and the azimuth Φ. Here the case Φ=0° is called "the left sun" and the title "the right sun" belongs to case Φ=180°, see Fig. 1; F_0 is irradiance of unit area perpendicular to the solar beam.

Functions $\sigma_{\mathrm{ext}}(x)$, $\sigma_{\mathrm{sca}}(x)$, $p(x,\chi)$ in each zone are assumed independent on height z

$$\sigma_{\mathrm{ext}}(x)=\begin{cases}\sigma_{\mathrm{ext},1} & \text{as } x<0,\\ \sigma_{\mathrm{ext},2} & \text{as } x>0,\end{cases}\qquad \sigma_{\mathrm{sca}}(x)=\begin{cases}\sigma_{\mathrm{sca},1} & \text{as } x<0,\\ \sigma_{\mathrm{sca},2} & \text{as } x>0,\end{cases}$$

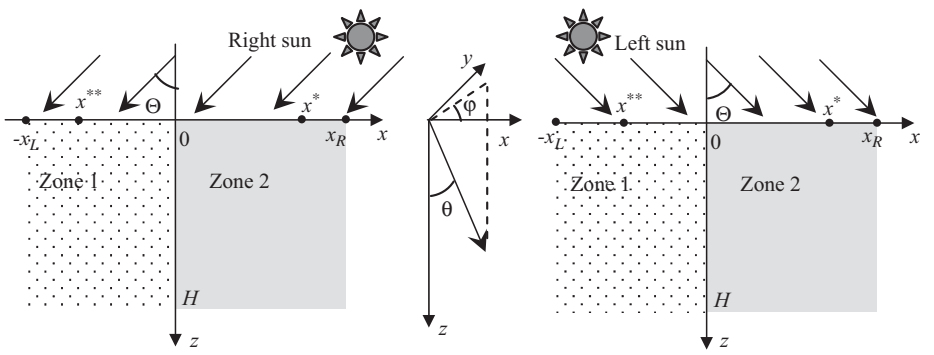

Fig. 1. The two-zone region.

$$p(x,\chi)=\begin{cases} p_1(\chi) & \text{as } x<0,\\ p_2(\chi) & \text{as } x>0. \end{cases}$$

Here x=0 is the coordinate of the vertical boundary of two regions with different optical properties.

The following boundary conditions are used together with Eq. (1)

$$I(x,0,\theta,\varphi)=0 \quad \text{as } \cos\theta>0, \tag{2}$$

$$I(x,H,\theta,\varphi)=0 \quad \text{as } \cos\theta<0, \tag{3}$$

$$I(x_R,z,\theta,\varphi)=I(x^*,z,\theta,\varphi) \quad \text{as } \cos\varphi<0, \tag{4a}$$

$$I(-x_L,z,\theta,\varphi)=I(x^{**},z,\theta,\varphi) \quad \text{as } \cos\varphi>0. \tag{4b}$$

Eqs. (2) and (3) are zero conditions at the bottom boundary $z=H$ and at the top boundary $z=0$.

Radiation intensity in a system of two large pixels is always independent on horizontal coordinate far from the zone boundary. The conditions (4) are imposed to guarantee this feature. For these purposes coordinates x^* и x^{**} in periodic conditions (4) should belong to points, put far away both the exterior boundaries $x=-x_L$, $x=x_R$ and the interior boundary $x=0$, see Fig. 1. We found that the sufficient distance is about 7 mean free photon path for the problem at hand.

3. M-1D simplified model

Because solution $I(x,z,\theta,\varphi)$ of the problem (1)–(4) is independent on the horizontal coordinate x far from the cloud edge, this function can be found via the 1D slab layer model at these remote points. The radiative transfer equation for this model can be written in the following way:

$$\gamma\frac{\partial I_k}{\partial z}+\sigma_{\text{ext},k}I_k(z,\theta,\varphi) = \frac{\sigma_{\text{sca},k}}{4\pi}\int_0^{\pi}\sin\theta'\,d\theta'\int_0^{2\pi} I_k(z,\theta',\varphi')\,p_k(\chi(\theta,\varphi,\theta',\varphi'))\,d\varphi' + Q_k(z,\theta,\varphi,\Theta,\Phi)F_0, \tag{5}$$

$$I_k(0,\theta,\varphi)=0 \quad \text{as } \cos\theta>0, \quad I_k(H,\theta,\varphi)=0 \quad \text{as } \cos\theta<0, \tag{6}$$

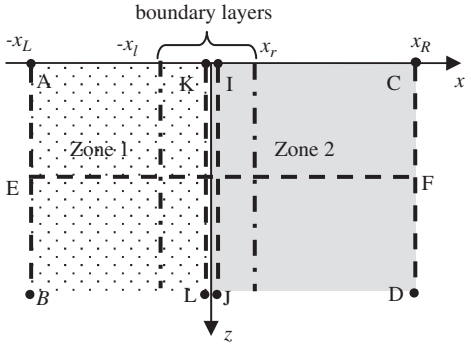

Fig. 2. Calculation lines within the two-zone region.

where k is the zone index. The solution of Eqs. (5) and (6) is carried out along lines AB and CD, see Fig. 2.

To find the horizontal distribution of the radiation intensity, we average 2D Eq. (1) over height z (see [3,4]). One has the following exact equation:

$$\xi\frac{\partial\bar I}{\partial x}+[\sigma_{\text{ext}}(x)+|\gamma|w(x,\theta,\varphi)]\bar I(x,\theta,\varphi) = \frac{\sigma_{\text{sca}}(x)}{4\pi}\int_0^{\pi}\sin\theta'\,d\theta'\int_0^{\pi}\bar I(x,\theta',\varphi')p(x,\chi(\theta,\varphi,\theta',\varphi'))\,d\varphi' + F_0\overline{Q}(x,\theta,\varphi,\Theta,\Phi) \tag{7}$$

for the averaged intensity

$$\bar I(x,\theta,\varphi)=\frac{1}{H}\int_0^H dz I(x,z,\theta,\varphi). \tag{8}$$

The positive weight function $w(x,\theta,\varphi)$ and effective source $\overline{Q}$ are defined by relations

$$w(x,\theta,\varphi)=I(x,\tilde z(\theta),\theta,\varphi)\Big/\int_0^H dz\,I(x,z,\theta,\varphi),$$
$$\tilde z(\theta)=\begin{cases} H & \text{as } \cos\theta>0,\\ 0 & \text{as } \cos\theta<0, \end{cases} \tag{9}$$

$$\overline{Q}(x,\theta,\varphi,\Theta,\Phi)=\frac{1}{H}\int_0^H dz\,Q(x,z,\theta,\varphi,\Theta,\Phi), \tag{10}$$

see Section 1 of Appendix A for details. Boundary conditions to Eq. (7) follow from the relations (4):

$$\bar I(x_R,\theta,\varphi)=\bar I(x^*,\theta,\varphi) \quad \text{as } \cos\varphi<0,$$
$$\bar I(-x_L,\theta,\varphi)=\bar I(x^{**},\theta,\varphi) \quad \text{as } \cos\varphi>0. \tag{11}$$

Eqs. (7)–(11) are solved along line EF, see Fig. 2.

The weight $w(x,\theta,\varphi)$, included into the effective extinction coefficient in Eq. (7), can be considered as some approximation to the relative value of the derivative of 2D solution over z. This weight is defined via solutions of the problems (5) and (6), if the point x is not close to the cloud edge x=0.

Vicinity of this boundary requires special care. We introduce boundary layers around plane x=0 by coordinates of their exterior boundaries $-x_\ell$ and x_r, see Fig. 2. The values x_ℓ and x_r can be obtained, for instance, as distances, at which source $\overline{Q}(x,\theta,\varphi,\Theta,\Phi)$ of the 1D problem (7)–(11) diminishes in e times under moving the plane x=0. In other words, values x_ℓ and x_r can be defined by the following equations:

$$\int_0^{\pi}d\theta\sin\theta\int_0^{2\pi}d\varphi\,\overline{Q}(0,\theta,\varphi,\Theta,\Phi)\Big/\int_0^{\pi}d\theta\sin\theta \times\int_0^{2\pi}d\varphi\,\overline{Q}(x_r,\theta,\varphi,\Theta,\Phi)=\exp(1), \tag{12a}$$

$$\int_0^{\pi}d\theta\sin\theta\int_0^{2\pi}d\varphi\,\overline{Q}(0,\theta,\varphi,\Theta,\Phi)\Big/\int_0^{\pi}d\theta\sin\theta \times\int_0^{2\pi}d\varphi\,\overline{Q}(-x_\ell,\theta,\varphi,\Theta,\Phi)=\exp(1). \tag{12b}$$

If the source $\overline{Q}(x,\theta,\varphi,\Theta,\Phi)$ in any boundary layer is strongly influenced by optical properties of a neighboring zone, in this layer the weight function $w(x,\theta,\varphi)$ of this

neighboring zone should be used. Such an influence is strong, when an optically thicker zone is illuminated from an optically thinner zone side. Thus, we can define the following values of the weight function $w(x,\theta,\varphi)$:

$$w(x,\theta,\varphi)=w_1(\theta,\varphi) \quad \text{as } x\le -x_\ell, \tag{13a}$$

$$w(x,\theta,\varphi)=\begin{cases} w_2(\theta,\varphi) & \tau_1\gg\tau_2 \text{ and } \Phi=180^\circ \\ w_1(\theta,\varphi) & \text{else} \end{cases} \quad \text{as } -x_\ell<x<0, \tag{13b}$$

$$w(x,\theta,\varphi)=\begin{cases} w_1(\theta,\varphi) & \tau_1\ll\tau_2 \text{ and } \Phi=0^\circ \\ w_2(\theta,\varphi) & \text{else} \end{cases} \quad \text{as } 0<x<x_r, \tag{13c}$$

$$w(x,\theta,\varphi)=w_2(\theta,\varphi) \quad \text{as } x\ge x_r, \tag{13d}$$

where τ_k is optically thickness of the k-th zone,

$$w_k(\theta,\varphi)=I_k(\tilde{z}(\theta),\theta,\varphi)\Big/\int_0^H dz I_k(z,\theta,\varphi) \tag{14}$$

is weight function defined by the intensity $I_k(z,\theta,\varphi)$ at the infinity in the k-th zone (when intensity is defined by the 1D problem (5) and (6)).

Besides, to reduce possible non-physical oscillations of the 1D solution of the problem (7)–(11), we impose restriction on "jump" of intensity at zones boundary

$$|\bar{I}(x+0,\theta,\varphi)-\bar{I}(x-0,\theta,\varphi)|\le J(\theta,\varphi). \tag{15}$$

Maximum jump value $J(\theta,\varphi)$ can be defined by solving 2D Eq. (1) at lines $x=\pm 0$ via the two-flux approximation

$$\frac{\partial I^+(z)}{\partial z}+\sigma_{\text{ext}}(x)I^+(z)=\sigma^+_{\text{sca}}(x)I^+(z)+\sigma^-_{\text{sca}}(x)I^-(z)+Q^+(z,\Theta,\Phi)F_0, \tag{16a}$$

$$-\frac{\partial I^-(z)}{\partial z}+\sigma_{\text{ext}}(x)I^-(z)=\sigma^+_{\text{sca}}(x)I^-(z)+\sigma^-_{\text{sca}}(x)I^+(z)+Q^-(z,\Theta,\Phi)F_0, \tag{16b}$$

see Section 2 of Appendix A for details. Here functions $I^+(z)$ and $I^-(z)$ correspond to intensities of radiation directed upward ($\gamma>0$) and downward ($\gamma<0$), values $\sigma^+_{\text{sca}}(x)$ and $\sigma^-_{\text{sca}}(x)$ are coefficients of scattering forward (by angle $<90^\circ$) and backward (by angle $>90^\circ$) correspondingly; sources terms $Q^+(z,\Theta,\Phi)$ and $Q^-(z,\Theta,\Phi)$ are mean values of the source $Q(x,z,\theta,\varphi,\Theta,\Phi)$ for $\gamma>0$ and $\gamma<0$ at a given point $x=\pm 0$

$$Q^+(z,\Theta,\Phi)=\frac{1}{2\pi}\int_0^{\pi/2}d\theta\sin\theta\int_0^{2\pi}d\varphi\,Q(x,z,\theta,\varphi,\Theta,\Phi), \tag{17a}$$

$$Q^-(z,\Theta,\Phi)=\frac{1}{2\pi}\int_{\pi/2}^{\pi}d\theta\sin\theta\int_0^{2\pi}d\varphi\,Q(x,z,\theta,\varphi,\Theta,\Phi). \tag{17b}$$

Boundary conditions to Eq. (16) follow from conditions (2) and (3)

$$I^+(0)=0, \quad I^-(H)=0. \tag{18}$$

The solution of the 1D problem (16), (18) is carried out for $x=\pm 0$ along lines KL and IJ, see Fig. 2.

Thus, the simplified M-1D algorithm to the problem (1)–(4) can be briefly outlined by the following steps:

- Calculation of radiation intensity at infinity ($x\to\pm\infty$) for each zone (functions $I_k(z,\theta,\varphi)$, k=1, 2) via solving the 1D problem (5) and (6).
- Determination of sizes x_r and x_ℓ of corresponding boundary layers via Eq. (12).
- Calculation of weight functions $w_k(\theta,\varphi)$ by Eq. (14).
- Determination of the weight function $w(x,\theta,\varphi)$ by expressions (13).
- Calculation of averaged source $\overline{Q}(x,\theta,\varphi,\Theta,\Phi)$ via equality (10).
- Determination of the maximum "jump" $J(\theta,\varphi)$ by solving the 1D problems (16)–(18).
- Calculation of averaged over height intensity $\bar{I}(x,\theta,\varphi)$ as solution of the 1D problem (7)–(11) under additional condition (15).
- Finding reflected radiation intensity at the top boundary x=0 by Eq. (9):

$$I(x,0,\theta,\varphi)|_{\cos\theta<0}=Hw(x,\theta,\varphi)\bar{I}(x,\theta,\varphi). \tag{19}$$

- Calculating the brightness coefficient

$$R(x)=\pi I(x,0,\pi,0)/[F_0\cos\Theta].$$

- Normalizing the brightness coefficient

$$\tilde{R}(x)=\begin{cases} R_1R(x)/R(-x_L) & \text{as } x<0, \\ R_2R(x)/R(x_R) & \text{as } x>0, \end{cases} \tag{20}$$

to compensate errors of approximations (19) caused by errors of weight function $w(x,\theta,\varphi)$ via the formulas (13) in vicinity of the media boundary. Value R_k in Eq. (20) is the brightness coefficient of the k-th zone, corresponding to radiation intensity at infinity (I_k).

This algorithm does avoid the solution of the 2D problem, but requires to solve five 1D problems. They are two problems (5) and (6), two problems (16)–(18) and one problem (7)–(11). The problems (5) and (6) and (16)–(18) are independent, whereas the effective extinction coefficient and solution jump restriction J in the problem (7)–(11) are defined via solutions of the problems (5) and (6) and (16)–(18). We solve all 1D problems via introduction of spatial and angular meshes and replacing the integro-differential equations by mesh approximations. The fast explicit sweep method is applied to the problems (16)–(18) (see Section 3 of Appendix A), whereas successive-orders-of-scattering (SOS) iteration process is used in the problems (5) and (6) and (7)–(11), (15). In addition, DSA technique (see [6,7]) to the SOS iteration acceleration in problems (5) and (6) is used. Computation time and cost reduction method are discussed in Section 4.

4. Numerical results

Let consider a simple model problem, where zone 1 is clear sky and zone 2 is cloud, see Fig. 1, under the

following parameters:

(a) height H=4 km,
(b) optical thickness of a clear sky $\tau_1 = 0.8262$,
(c) optical thickness of a cloud $\tau_2 = \tau_{\text{cloud}} \gg \tau_1$,
(d) single scattering albedo for both zones $\omega_0 \in (0, 1)$ (so we assumed that both cloud and clear sky contain some absorber of incident radiation).

Here τ_{cloud} and ω_0 are being varied values.

Scattering phase functions for both cloud and aerosol were obtained via the Mie theory [8] at the wavelength 412 nm. In the case of cloud we have used Deirmendjian's Cloud_C1 model and for the aerosol the standard oceanic atmospheric aerosol model is used (see [9,10]). The molecular scattering but not absorption was taken into account. The peaks of the phase functions of cloud and aerosol particles were replaced by the delta-function via delta–M method [11], and the regular components are decomposed into P_{33} Legendre series.

Computations were run for two azimuths Φ=0° and 180° and some zenith angles. The code RADUGA, based upon mesh schemes of the discrete ordinate method (see details in [12]) is used to 2D calculations, whereas new special code runs for M-1D problems. The results (brightness coefficients), found via both the exact 2D problem (1)–(4) and also the presented M-1D method and IPA model for zenith angles Θ=20°, 40°, 60° and parameters $\tau_{\text{cloud}} = 10$, $\omega_0 = 0.995$, are given in Figs. 3–5.

One can see that the presented M-1D algorithm in contrast to IPA yields spatial distribution of brightness coefficient in a vicinity of the cloud edge, which well coincides with results derived by the exact 2D equation. In particular, the M-1D algorithm gives an opportunity to

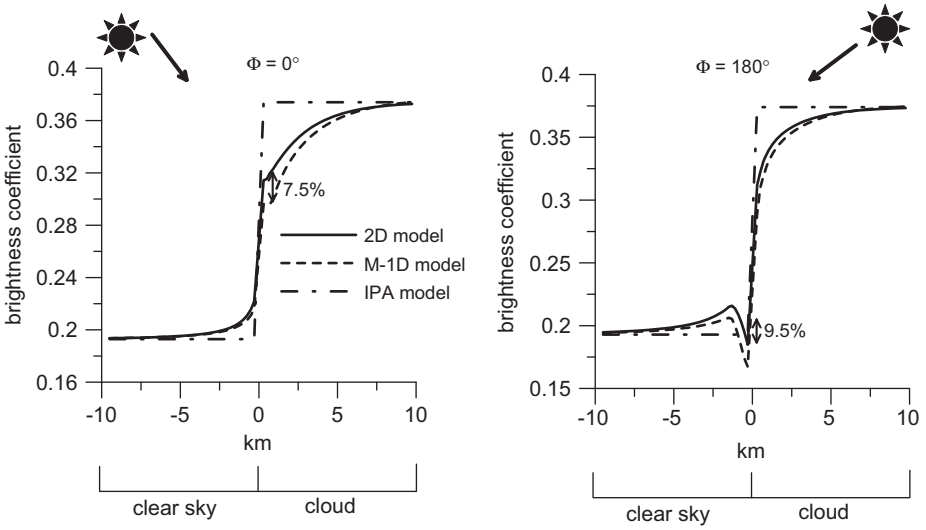

Fig. 3. Brightness coefficient as the function of the horizontal coordinate at Θ=20°, $\tau_{\text{cloud}} = 10$, $\omega_0 = 0.995$.

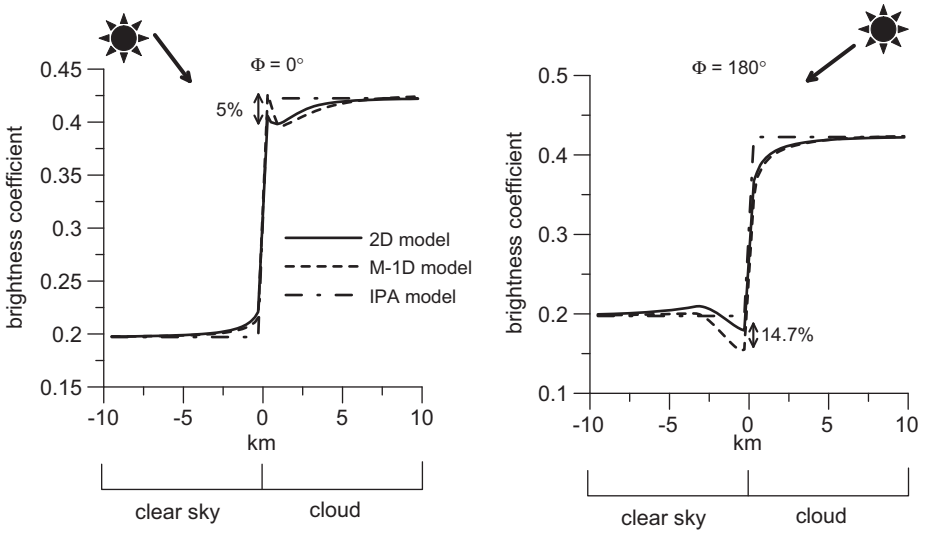

Fig. 4. Brightness coefficient as the function of the horizontal coordinate at Θ=40°, $\tau_{\text{cloud}} = 10$, $\omega_0 = 0.995$.

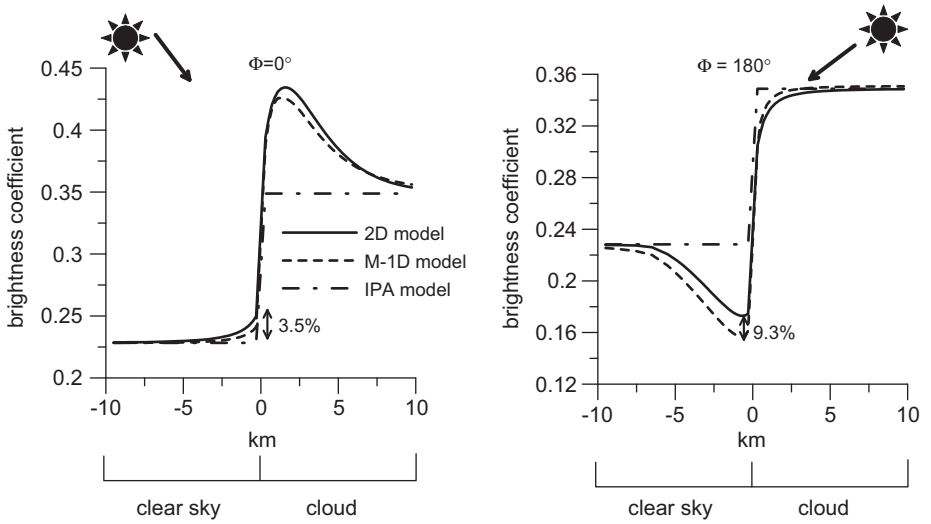

Fig. 5. Brightness coefficient as the function of the horizontal coordinate at Θ=60°, $\tau_{cloud}=10$, $\omega_0=0.995$.

Table 1
Relative errors (%) of the M-1D algorithm at $\tau_{cloud}=5$, $\omega_0=0.99$.

Zenith angle Θ (deg)	Φ=180° (illumination from the right)		Φ=0° (illumination from the left)	
	Zone 1 (clear sky)	Zone 2 (cloud)	Zone 1 (clear sky)	Zone 2 (cloud)
10	1.73	3.58	0.64	6.54
20	6.71	2.85	0.51	4.42
30	10.90	1.40	0.15	2.10
40	13.69	0.64	0.16	3.85
50	14.10	1.81	0.55	2.77
60	11.54	3.93	1.83	6.68

Table 2
Relative errors (%) of the M-1D algorithm at $\tau_{cloud}=10$, $\omega_0=0.99$.

Zenith angle Θ (deg)	Φ=180° (illumination from the right)		Φ=0° (illumination from the left)	
	Zone 1 (clear sky)	Zone 2 (cloud)	Zone 1 (clear sky)	Zone 2 (cloud)
10	5.40	7.66	1.33	7.53
20	10.62	7.27	2.37	7.84
30	13.60	6.18	2.39	2.74
40	14.53	5.53	2.57	5.66
50	13.30	3.23	2.96	1.39
60	9.34	2.53	3.59	2.90

Table 3
Relative errors (%) of the M-1D algorithm at $\tau_{cloud}=10$, $\omega_0=0.995$.

Zenith angle Θ (deg)	Φ=180° (illumination from the right)		Φ=0° (illumination from the left)	
	Zone 1 (clear sky)	Zone 2 (cloud)	Zone 1 (clear sky)	Zone 2 (cloud)
10	5.33	8.01	1.43	7.88
20	10.69	7.69	2.49	8.05
30	13.71	6.75	2.47	3.17
40	14.68	6.21	2.59	4.36
50	13.31	3.91	2.97	2.15
60	9.29	2.04	3.61	3.21

Table 4
Relative errors (%) of the M-1D algorithm at parameters $\tau_{cloud} = 15$, $\omega_0 = 0.99$.

Zenith angle Θ (deg)	Φ=180° (illumination from the right)		Φ=0° (illumination from the left)	
	Zone 1 (clear sky)	Zone 2 (cloud)	Zone 1 (clear sky)	Zone 2 (cloud)
10	6.61	9.16	2.71	6.92
20	11.03	9.43	4.30	5.96
30	12.71	8.84	4.56	2.57
40	12.81	8.33	4.76	10.9
50	10.96	5.49	5.52	6.20
60	7.33	2.64	6.18	5.38

Table 5
Summary values of coefficients of brightness of reflected light over boundaries layers at the azimuth Φ=0°.

Zenith angle Θ (deg)	r_1 (clear sky)			r_2 (cloud)		
	2D	M-1D	IPA	2D	M-1D	IPA
10	0.340	0.338	0.311	1.049	1.015	1.172
20	0.295	0.290	0.270	1.076	1.025	1.197
30	0.258	0.254	0.238	0.989	0.964	1.086
40	0.255	0.250	0.237	0.480	0.485	0.507
60	0.223	0.218	0.207	0.970	0.964	0.938

Table 6
Summary values of coefficients of brightness of reflected light over boundaries layers at the azimuth Φ=180°.

Zenith angle Θ (deg)	r_1 (clear sky)			r_2 (cloud)		
	2D	M-1D	IPA	2D	M-1D	IPA
10	0.552	0.540	0.505	0.793	0.769	0.879
20	0.660	0.629	0.618	0.679	0.657	0.748
30	0.743	0.692	0.714	0.565	0.549	0.620
40	0.754	0.687	0.750	0.465	0.453	0.507
50	0.445	0.393	0.498	0.327	0.324	0.361
60	0.919	0.851	1.096	0.254	0.257	0.279

find maxima of brightness (*brightening effects*) at the clouds edges and minima of brightness (*shadowing effects*) in clear sky close to clouds edges, existing due to the horizontal radiation transport caused by "jump" of optical properties of the media.

The maximum relative errors (%) of the M-1D algorithm are given in Tables 1–4. One can see that errors for all cases considered are in the range 1–15% in the vicinity of the cloud boundary depending on illumination conditions and optical parameters.

The integrated values of coefficients of brightness of reflected light defined as

$$r_1 = \int_{-s_\ell}^{0} dx\, R(x), \quad r_2 = \int_{0}^{s_r} dx\, R(x),$$

obtained via 2D, M-1D and IPA models, are presented for different azimuth and zenith angles in Tables 5 and 6. Boundary layer sizes s_ℓ, s_r are obtained as distances at which relative differences between brightness coefficients and their values at infinity

$$\varepsilon(x) = \begin{cases} 100|1 - R(x)/R(-x_L)|\% & \text{as } x < 0, \\ 100|1 - R(x)/R(x_R)|\% & \text{as } x > 0 \end{cases}$$

$< 5\%$. 2D brightness coefficients are used for relative differences calculations.

The data presented in Tables 5 and 6 show that the values r_1 and r_2 are generally smaller for M-1D model than for the IPA model, especially for the left sun.

Finally, one needs to pay attention to the computation cost reduction due to replacing 2D method via M-1D technique. The reduction degree depends strongly on numerical methods to solve 2D and M-1D equations. If the discrete ordinate method and SOS iterations are used for both 2D and M-1D problems, then reduction degree is about 17 for all studied cases (for the same standard PC). This acceleration is only owing to replacing 2D problems by 1D equations. More acceleration can be achieved via more rapid method to solve M-1D problems, which are not applicable to 2D and 3D problems. They are analytical methods (for example, [13,14]) which based on analytical solutions of the discrete ordinate differential equation systems. Then the computation cost reduction degree is even larger.

5. Conclusion

The simplified M-1D algorithm to simulate horizontal distributions of coefficient of the reflected light brightness in regions composed of two large zones with different optical properties is presented. The algorithm is based on the solution of five 1D problems without using the 2D time-consuming transport codes and any assumptions on both optical properties of zones and diffuse radiation intensity. The derived 1D problems can be solved using any available 1D method.

By means of the presented method brightness coefficients with typical multi-dimensional effects (brightening and shadowing) in model problems are obtained with relative errors $< 5\%$ depending on the illumination conditions and optical parameters of studied regions.

It should be stressed that we used the mesh approximations of the discrete ordinate method and iterative processes to carry out 1D calculations. However, runtime can be significantly reduced via the usage of high accuracy analytical techniques for these computations. At the same

time there are not fast analytical methods for the 2D transport equation solution.

The M-1D algorithm solves the radiative transfer equation for the medium composed of two large homogeneous zones (clear sky and cloud). But it is possible to extend the technique using the idea presented here to systems with arbitrary number of homogeneous zones (e.g., broken cloud fields). In such a case M-1D method must be based on 3^*N-1 1D-equations, where N is number of zones. Direct extension of the suggested method to 3D geometry leads to systems of 1D and 2D equations in natural way.

The basic condition to applicability of this M-1D method is large optical widths of pixels. This condition gives an opportunity to find the effective extinction coefficient in the modified 1D equation, defining horizontal distribution of radiation intensity, with sufficient accuracy by means of height distribution of the radiation intensity in infinity of an each zone, found via the 1D slab model. This technique is not applicable for systems of narrow pixels (both 2D and 3D), where another approach is desired (currently under development in our group).

Acknowledgments

The work is supported by research program N 14 of Presidium of Russian Academy of Sciences. Alexander Kokhanovsky thanks German Science Foundation (DFG) for support of his research via the Project BU 688/18-1 "Terra".

Appendix A. Theoretical basis of the approximate model

In this section some details of the model construction are given.

1. To find Eq. (7), we averaged Eq. (1) over height z. Based on definitions (8) and (10), one arrives at

$$\xi\frac{\partial\bar{I}}{\partial x}+\sigma_{\text{ext}}(x)\bar{I}(x,\theta,\varphi)+\frac{\gamma}{H}[I(x,H,\theta,\varphi)-I(x,0,\theta,\varphi)]$$
$$=\frac{\sigma_{\text{sca}}(x)}{4\pi}\int_0^{\pi}\sin\theta'\,d\theta'\int_0^{2\pi}\bar{I}(x,\theta',\varphi')p(x,\chi(\theta,\varphi,\theta',\varphi'))\,d\varphi'$$
$$+F_0\overline{Q}(x,\theta,\varphi,\Theta,\Phi). \quad (A.1)$$

The transformation of the third term on the left side of this equation is carried out by the boundary conditions (2) and (3). It follows:

$$\frac{\gamma}{H}[I(x,H,\theta,\varphi)-I(x,0,\theta,\varphi)]=\frac{\gamma}{H}I(x,H,\theta,\varphi)\quad\text{as }\gamma\cos\theta>0,$$

$$\frac{\gamma}{H}[I(x,H,\theta,\varphi)-I(x,0,\theta,\varphi)]=\frac{-\gamma}{H}I(x,0,\theta,\varphi)\quad\text{as }\gamma\cos\theta<0.$$

Using the definition (9), one finds the relation

$$\frac{\gamma}{H}[I(x,H,\theta,\varphi)$$
$$-I(x,0,\theta,\varphi)]=\frac{|\gamma|}{H}I(x,\tilde{z}(\theta),\theta,\varphi)=|\gamma|w(x,\theta,\varphi)\bar{I}(x,\theta,\varphi).$$

Substituting this equality in (A.1) one obtains Eq. (7). There is no approximation in (7) under exact weight $w(x,\theta,\varphi)$.

2. To construct Eq. (16), first we let the angle θ be equal to 0 and π in Eq. (1):

$$\frac{\partial I(x,z,0,\varphi)}{\partial z}+\sigma_{\text{ext}}(x)I(x,z,0,\varphi)$$
$$=\frac{1}{4\pi}\sigma_{\text{sca}}(x)\int_0^{\pi}\sin\theta'\,d\theta'\int_0^{2\pi}I(x,z,\theta',\varphi')p(x,\cos\theta')\,d\varphi'$$
$$+Q(x,z,0,\varphi,\Theta,\Phi)F_0, \quad (A.2)$$

$$-\frac{\partial I(x,z,\pi,\varphi)}{\partial z}+\sigma_{\text{ext}}(x)I(x,z,\pi,\varphi)$$
$$=\frac{1}{4\pi}\sigma_{\text{sca}}(x)\int_0^{\pi}\sin\theta'\,d\theta'\int_0^{2\pi}I(x,z,\theta',\varphi')p(x,-\cos\theta')\,d\varphi'$$
$$+Q(x,z,\pi,\varphi,\Theta,\Phi)F_0. \quad (A.3)$$

Secondly, we introduce the following approximate relations:

$$I(x,z,\theta,\varphi)|_{0<\theta<\pi/2}\approx\frac{1}{2\pi}\int_0^{\pi/2}d\theta'\sin\theta'\int_0^{2\pi}d\varphi'\,I(x,z,\theta',\varphi')$$
$$=I^+(x,z),$$

$$I(x,z,\theta,\varphi)|_{\pi/2<\theta<\pi}\approx\frac{1}{2\pi}\int_{\pi/2}^{\pi}d\theta'\sin\theta'\int_0^{2\pi}d\varphi'\,I(x,z,\theta',\varphi')$$
$$=I^-(x,z).$$

The integrals on the right sides of (A.2), (A.3) can be presented as

$$\frac{1}{4\pi}\sigma_{\text{sca}}(x)\int_0^{\pi}\sin\theta'\,d\theta'\int_0^{2\pi}I(x,z,\theta',\varphi')p(x,\pm\cos\theta')\,d\varphi'$$
$$=\frac{1}{2}\sigma_{\text{sca}}(x)[I^+(x,z)\int_0^{\pi/2}d\theta'\sin\theta'p(x,\pm\cos\theta')$$
$$+I^-(x,z)\int_{\pi/2}^{\pi}d\theta'\sin\theta'p(x,\pm\cos\theta')]=\sigma^{\pm}_{\text{sca}}(x)I^+(x,z)$$
$$+\sigma^{\mp}_{\text{sca}}(x)I^-(x,z),$$

where

$$\sigma^+_{\text{sca}}(x)=\frac{1}{2}\sigma_{\text{sca}}(x)\int_0^{\pi/2}d\theta'\sin\theta'p(x,\cos\theta')$$
$$=\frac{1}{2}\sigma_{\text{sca}}(x)\int_{\pi/2}^{\pi}d\theta'\sin\theta'p(x,-\cos\theta'), \quad (A.4)$$

$$\sigma^-_{\text{sca}}(x)=\frac{1}{2}\sigma_{\text{sca}}(x)\int_{\pi/2}^{\pi}d\theta'\sin\theta'p(x,\cos\theta')$$
$$=\frac{1}{2}\sigma_{\text{sca}}(x)\int_0^{\pi/2}d\theta'\sin\theta'p(x,-\cos\theta') \quad (A.5)$$

are the coefficients of scattering (forward and backward, respectively). Replacing source terms in Eqs. (A.2), (A.3) by approximate relations

$$Q(x,z,0,\varphi,\Theta,\Phi)$$
$$\approx Q^+(z,\Theta,\Phi),\quad Q(x,z,\pi,\varphi,\Theta,\Phi)\approx Q^-(z,\Theta,\Phi),$$

where the functions $Q^{\pm}(z,\Theta,\Phi)$ are defined via Eq. (17) and substituting the equalities (A.4), (A.5) into Eqs. (A.2) and (A.3), we derive Eq. (16).

3. The numerical method for the solution of the system (16) of two linear differential equations is based upon a

mesh scheme of the second order of accuracy:

$$\frac{I^+(z_{k+1/2})-I^+(z_{k-1/2})}{z_{k+1/2}-z_{k-1/2}}+(\sigma_{\rm ext}(x)-\sigma^+_{\rm sca}(x))\frac{I^+(z_{k+1/2})+I^+(z_{k-1/2})}{2}$$

$$=\sigma^-_{\rm sca}(x)\frac{I^-(z_{k+1/2})+I^-(z_{k-1/2})}{2}+Q^+(z_k,\Theta,\Phi)F_0, \qquad (A.6)$$

$$-\frac{I^-(z_{k+1/2})-I^-(z_{k-1/2})}{z_{k+1/2}-z_{k-1/2}}+(\sigma_{\rm ext}(x)$$
$$-\sigma^+_{\rm sca}(x))\frac{I^-(z_{k+1/2})+I^-(z_{k-1/2})}{2}$$
$$=\sigma^-_{\rm sca}(x)\frac{I^+(z_{k+1/2})+I^+(z_{k-1/2})}{2}+Q^-(z_k,\Theta,\Phi)F_0. \qquad (A.7)$$

Here $x=0^+$ or $x=0^-$, $z_{k+1/2}$, $k=1,\ldots,K$, are edges of cells of a possibly irregular mesh over height z, $z_{1/2}=0$, $z_{K+1/2}=H$, $z_k=(z_{k+1/2}+z_{k-1/2})/2$ are centers of cells. The boundary conditions for the system (A.6), (A.7) follow from the conditions (18):

$$I^+(z_{1/2})=0, \quad I^-(z_{K+1/2})=0. \qquad (A.8)$$

The linear algebraic system (A.6)–(A.8) is resolved by fast explicit sweep method, version of the explicit Gauss's method [15].

References

[1] Marshak A, Davis A. 3D radiative transfer in cloudy atmospheres (Physics of Earth and Space Environments). Berlin: Springer; 2002.

[2] Iwabuchi H. Retrieval of cloud optical thickness and effective radius using multispectral remote sensing and accounting for 3D effects. In: Kokhanovsky AA, editor. Light scattering reviews, vol. 2. Berlin: Springer; 2007. p. 97–124.

[3] Nikolaeva OV. Simplified 1D model to 2D transport equation. In: Proceedings of 20th international conference on transport theory, Obninsk, 2007.

[4] Bass LP, Germogenova TA, Nikolaeva OV, Kokhanovsky AA, Kuznetsov VS. Numerical simulation of boundary effects in aerosol and cloud optics. Atmos Oceanic Opt 2009;22:102–7.

[5] Marshak A, Davis A, Cahalan R, Wiscombe W. Nonlocal independent pixel approximation: direct and inverse problems. IEEE Trans Geosci Remote Sensing 1998;36:192–208.

[6] Marchuk GI, Lebedev VI. Numerical methods in the theory of neutron transport. Amsterdam: OPA; 1986.

[7] Larsen EW. Unconditionally stable diffusion-synthetic acceleration methods for the slab geometry discrete-ordinates equations. Part I: theory. Nucl Sci Eng 1982;82:47–63.

[8] van de Hulst HC. Multiple light scattering. New York: Academic Press; 1980.

[9] Kokhanovsky AA. Cloud optics. Berlin: Springer; 2006.

[10] Kokhanovsky AA. Aerosol optics. Berlin: Springer; 2008.

[11] Wiscombe WJ. The delta–M method: rapid yet accurate radiative flux calculations for strongly asymmetric phase functions. J Atmos Sci 1977;34:1408–22.

[12] Nikolaeva OV, Bass LP, Germogenova TA, Kokhanovsky AA, Kuznetsov VS, Mayer B. The influence of neighboring clouds on the clear sky reflectance studied with the 3-D transport code RADUGA. JQSRT 2005;94:405–24.

[13] Lenoble J, editor. Standart procedure to compute atmospheric radiative transfer in a scattering atmosphere. Boulder, CO: National Center for Atmospheric Research; 1977.

[14] Chalhoub ES, Campos Velho HF, Garcia RDM, Vilhena VT. A comparison of radiances generated by selected methods of solving the radiative-transfer equation. Transp Theory Stat Phys 2003;32:473–503.

[15] Samarskii AA, Nikolaev ES. Numerical methods for grid equations. Basel: Verlag; 1989.